ChemComm

COMMUNICATION

View Article Online
View Journal | View Issue

Cite this: *Chem. Commun.*, 2014, **50**, 12462

Received 29th July 2014,
Accepted 27th August 2014

DOI: 10.1039/c4cc05896h

www.rsc.org/chemcomm

High performance, air stable n-type single crystal transistors based on core-tetrachlorinated perylene diimides†

Chunming Liu, Chengyi Xiao, Yan Li,* Wenping Hu, Zhibo Li and Zhaohui Wang*

Organic single crystal transistors based on two kinds of core-tetrachlorinated perylene diimides (4ClPDIs) are fabricated. Compared with alkyl substituted 4ClPDI, the transistors based on fluoroalkyl substituted 4ClPDI exhibit an air-stable electron mobility of up to 1.43 $cm^2 V^{-1} s^{-1}$ and high photocurrent with an on/off ratio of 1000, which are associated with its close packing arrangement.

Over the past decade, organic field-effect transistors (OFETs) based on high performance organic semiconductors have received significant attention because of their potential applications in electronics.[1] To this end, a number of organic p-type semiconductors with high hole mobilities have been developed.[2] However, organic n-type semiconductors with high electron mobilities in air are still limited because of the lack of good n-type molecular skeletons and insufficient understanding of the structure–property relationship. Organic single crystals are usually regarded as important candidates for the fabrication of high performance devices due to their perfectly ordered molecules, absence of grain boundaries and minimized concentration of charge traps.[3] Thus the single crystal transistors provide an opportunity to reveal the intrinsic structure–property relationship, which provides guidance in the rational design of high performance n-type organic semiconducting materials.

Perylene diimides (PDIs) are regarded as one of the most promising n-type semiconductors due to their accessibility, high electron affinity, and the tunability of optical and electronic properties.[4] Chemical modifications both at the imide groups and in the bay regions of PDIs are regarded as successful synthetic strategies.[5] Recently, a high-mobility, air-stable n-type organic semiconductor based on core-tetrachlorinated perylene diimide (4ClPDI) was reported, though it had poor solubility and was purified by consecutive vacuum sublimations due to the presence of free NH imide groups.[6] Meanwhile, a new PDI derivative, named C12-4CldiPDI, was also reported by our group, which exhibits excellent n-type transistor behaviour even in air.[7] Considering the accessibility and solubility, herein we focus on the single crystal devices of two different alkyl substituted 4ClPDIs and aim at probing the influence of different alkyl substitutions on the molecular arrangement and photoelectric performance.

The single crystals of fluoroalkyl and alkyl substituted 4ClPDIs, named C8F-4ClPDI and C8-4ClPDI (Fig. 1a), were grown using the physical vapor transport (PVT) method in a three-zone horizontal-tube furnace. A quartz boat with the sample powder was placed in the high temperature zone (220 °C for C8F-4ClPDI and 250 °C for C8-4ClPDI) with high-purity argon being used as carrier gas (100 mL min^{-1}). Inerratic micrometer-sized crystal ribbons were slowly grown on an octadecyltrichlorosilane (OTS)-modified Si/SiO_2 substrate in a relatively lower-temperature zone. Fig. 1b and c show low-magnification optical microscopy (OM) images of microribbons and individual crystal scanning electron microscopy (SEM) images. The single-crystal microribbons of both

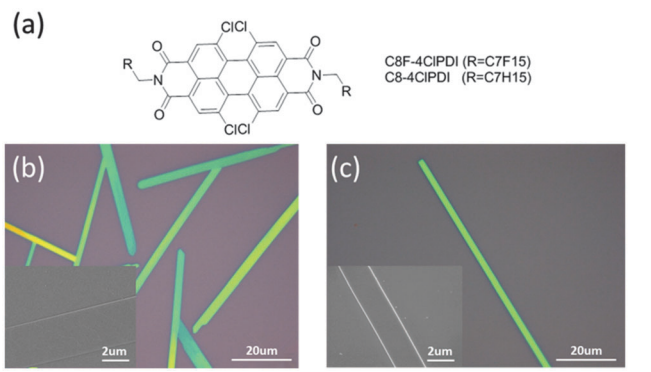

Fig. 1 (a) Molecular structure of two different core-tetrachlorinated perylene diimides. (b) OM and SEM images of single crystal microribbons of C8F-4ClPDI. (c) OM and SEM images of single crystal microribbons of C8-4ClPDI.

Beijing National Laboratory for Molecular Sciences, Key Laboratory of Organic Solids, Institute of Chemistry, Chinese Academy of Sciences, Beijing 100190, P. R. China. E-mail: wangzhaohui@iccas.ac.cn, yanli@iccas.ac.cn; Fax: +86-10-62653617; Tel: +86-10-62653617

† Electronic supplementary information (ESI) available: Intermolecular interaction image, OM image of transistor with four electrodes, statistical mobility distributions, *I–V* curves, and crystal data for C8F-4ClPDI. CCDC 1016715. For ESI and crystallographic data in CIF or other electronic format see DOI: 10.1039/c4cc05896h

C8F-4ClPDI and C8-4ClPDI exhibit excellent long range regularity with a length of 10 to 100 micrometers and the thickness ranging from several nanometers to tens of nanometers. The surfaces of these microribbons are very smooth and are grown in parallel with the substrate.

For better understanding the molecular arrangement in single-crystal microribbons, crystals suitable for single-crystal X-ray analysis are obtained by slow evaporation of chloroform solution of C8F-4ClPDI. The X-ray data reveal that the crystal of C8F-4ClPDI belongs to the monoclinic crystal system, and the *a*-axis is oriented perpendicularly to the substrate while the *b*–*c* plane (the carrier conduction path) is arranged parallel to the substrate. The crystal structure is shown in Fig. 2a and a highly twisted molecular core can be seen. The crystal packing arrangements are shown in Fig. 2b and Fig. S1 (ESI†), which reveal that the molecules are arranged in columnar stacks along the *c*-axis and as lamellar structures along *a*-axis. What should be mentioned is that except for the compact stacks formed during the distorted molecular skeletons, there are many F···F and F···H interactions during the alternately overlapped fluorinated alkyl chains which may effectively prevent the intrusion of H_2O and O_2 in air (Fig. S1, ESI†).

The transmission electron microscopy (TEM) image of a representative single-crystalline microribbon and selected area electron diffraction (SAED) pattern obtained from the same microribbon are shown in Fig. 3a and b. The powder X-ray diffraction (XRD) pattern and the atomic force microscopy (AFM) are shown in Fig. 3c and d. We can learn from the AFM images of C8F-4ClPDI that the thickness of each layer of the single crystal microribbon is 20.6 Å, corresponding to the length of the distorted molecular core and a fluorinated alkyl chain. This result is consistent with the XRD data (*d* spacing 20.1 Å) (Fig. 3c). The TEM image of C8F-4ClPDI reveals that the single-crystal microribbon exhibits a very

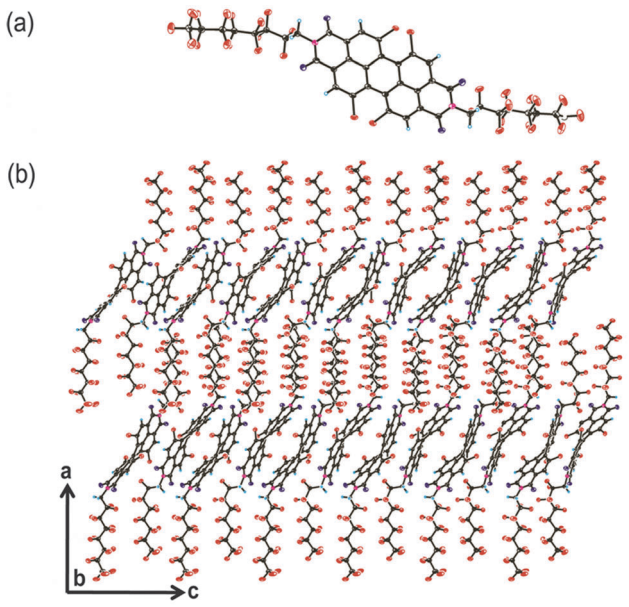

Fig. 2 (a) X-ray crystallographic structure of C8F-4ClPDI. (b) Molecular arrangement in the *a*–*c* plane.

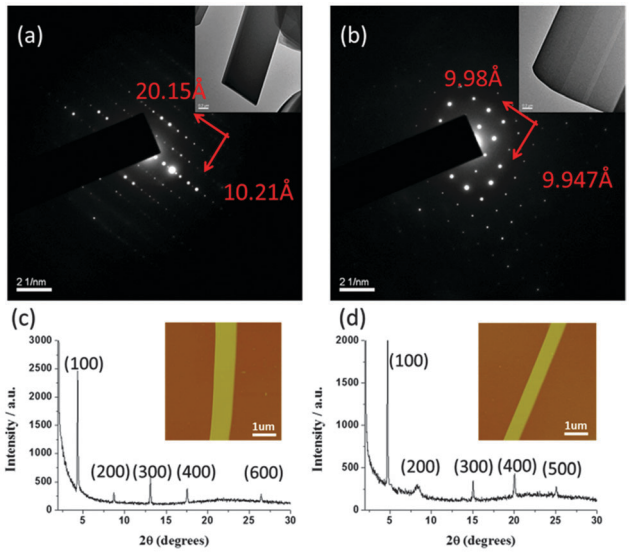

Fig. 3 (a) TEM image of C8F-4ClPDI microribbon and its corresponding SAED pattern. (b) TEM image of C8-4ClPDI microribbon and its corresponding SAED pattern. (c) XRD pattern and AFM image of C8F-4ClPDI single crystal microribbon. (d) XRD pattern and AFM image of C8-4ClPDI single crystal microribbon.

neat morphology and the corresponding electron diffraction patterns all show sharp and well-defined diffraction spots (Fig. 3a). AFM and XRD images in Fig. 3d demonstrate that the single-crystal microribbon of C8-4ClPDI also has a lamellar structure, and the thickness of each layer is about 19.3 Å. TEM and SAED images (Fig. 3b) combined with XRD data demonstrate that the single-crystal microribbon of C8-4ClPDI grows along the π–π stacking direction.[8] Well-defined and bright diffraction spots were also found in different regions, confirming the single-crystal structure of the C8-4ClPDI microribbon.[9] Both compounds C8F-4ClPDI and C8-4ClPDI can generate highly-crystalline layered structures which may be beneficial for charge transport in single-crystal microribbons. The XRD images and SAED patterns of two compounds are very similar. So we speculate that the two compounds have a similar molecular arrangement in single-crystal microribbons.

Subsequently, transistors based on single-crystal microribbons of C8F-4ClPDI and C8-4ClPDI were fabricated using a doped n-type silicon wafer as the gate electrode, Au as the source and drain electrodes, and OTS-modified SiO_2 as the dielectric layer. Firstly, single-crystal microribbons of C8F-4ClPDI or C8-4ClPDI were deposited on an OTS/SiO_2/Si substrate using the PVT method. These single-crystal microribbons are all thin enough to minimize the effect of the resistance.[10] Secondly, by skillfully using our mechanical technique named the "pick and paste" method we pasted the Au electrodes directly onto crystals to avoid the thermal radiation.[11] The OFET devices fabricated were oriented along the growth direction of the single crystal microribbons and were all measured under ambient conditions. The transistors based on C8F-4ClPDI exhibit a typical n-type semiconducting behavior with an average electron mobility of 1.14 $cm^2\ V^{-1}\ s^{-1}$, the highest electron mobility of 1.43 $cm^2\ V^{-1}\ s^{-1}$, and an on/off ratio of $\sim 10^7$. The representative output and transfer characteristics

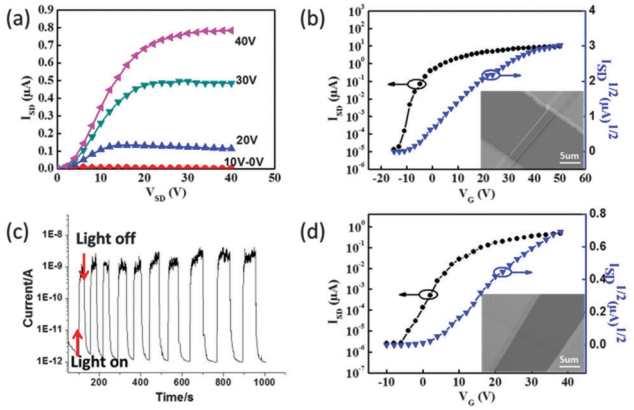

Fig. 4 (a) Output and (b) transfer characteristics of the representative single crystal device based on C8F-4ClPDI. Inset shows the SEM image of the single crystal device. (c) Photoresponsive behavior of a two-end single-crystalline device (white light, 3.76 mw cm^{-2}, an applied bias voltage −10 V). (d) Transfer characteristics of a single crystal device based on C8-4ClPDI. Inset shows the SEM image of the single crystal device.

of the transistors based on C8F-4ClPDI are plotted in Fig. 4a and b. Meanwhile, the anisotropic charge transport in the elongated crystals of C8F-4ClPDI is also explored by using an "organic nanowire mask" (Fig. S2, ESI†). It can be seen that the carrier mobility along the *c*-axis is far higher than that along the *b*-axis, which is attributed to the close molecular packing arrangement along the *c*-axis. For comparison, single-crystal transistors based on C8-4ClPDI exhibit relatively low mobility along the growth direction with the highest electron mobility of 0.8 cm^2 V^{-1} s^{-1} and an on/off ratio of 10^5. The performance of devices based on C8-4ClPDI attenuates very fast in air. Hence the output curve is unavailable and the transfer characteristics are plotted in Fig. 4d. Considering the different electron mobilities and stabilities of transistors based on C8F-4ClPDI and C8-4ClPDI, we speculate that the introduction of fluorinated alkyl chains into the imide groups lead to a more close-knit arrangement in the crystal structure. On the one hand, this tight arrangement is advantageous for the charge transfer in C8F-4ClPDI based devices.[12] On the other hand, the closely ordered crystal structure protects against the entry of water and oxygen molecules in air.[13]

To further explore the potential applications of C8F-4ClPDI in optoelectronic devices, the optical performance of the switching of white light was performed. The two-end crystal devices based on C8F-4ClPDI were fabricated using the "organic nanowire mask" technique in order to make a better contact with the electrode. It was concluded that the single-crystal devices of C8F-4ClPDI exhibit remarkably high sensitivity to light. The change in the current of the single-crystal devices in the dark and under white light illumination is plotted in Fig. 4c and Fig. S4 (ESI†). The photocurrent is found to switch promptly upon turning the white light on and off. Moreover, the dark current is only 1.18×10^{-12} A. Upon a white light illumination of 3.76 mw cm^{-2}, the photocurrent could approach 1.52×10^{-9} A, indicating an on/off ratio exceeding 1000 and an average light responsivity of 2.5 A W^{-1}. At the same time, the light response of C8-4ClPDI is poor and the current changes little when the white light is turned on and off.

In summary, organic single-crystal microribbons of two kinds of core-tetrachlorinated perylene diimides are produced using the physical vapor transport method, and transistors based on individual crystals are fabricated. Compared with C8-4ClPDI, the transistors based on C8F-4ClPDI exhibit an electron mobility of up to 1.43 cm^2 V^{-1} s^{-1} in air and an on/off ratio of 10^7, which are associated with its close packing arrangement not only for the distorted molecular skeletons but also for the alternately overlapped fluorinated alkyl chains. Moreover, the two-end single-crystal devices based on C8F-4ClPDI show remarkably high sensitivity to light with an on/off ratio of 1000. The comparative results may provide guidance for the rational design of high performance n-type organic semiconducting materials in the future.

We thank the National Natural Science Foundation of China (21225209, 21204091, 91027043 and 21190032), the 973 Program (2012CB932903), and the Chinese Academy of Sciences (XDB12010100) for financial support of this research.

Notes and references

1 (*a*) C. Wang, H. Dong, W. Hu, Y. Liu and D. Zhu, *Chem. Rev.*, 2012, **112**, 2208; (*b*) W. Jiang, Y. Li and Z. Wang, *Chem. Soc. Rev.*, 2013, **42**, 6113; (*c*) A. N. Sokolov, B. C.-K. Tee, C. J. Bettinger, J. B.-H. Tok and Z. Bao, *Acc. Chem. Res.*, 2012, **45**, 361.
2 (*a*) M. Gsänger, E. Kirchner, M. Stolte, C. Burschka, V. Stepanenko, J. Pflaum and F. Würthner, *J. Am. Chem. Soc.*, 2014, **136**, 2351; (*b*) X.-Y. Wang, F.-D. Zhuang, R.-B. Wang, X.-C. Wang, X.-Y. Cao, J.-Y. Wang and J. Pei, *J. Am. Chem. Soc.*, 2014, **136**, 3764.
3 R. W. I. de Boer, M. E. Gershenson, A. F. Morpurgo and V. Podzorov, *Phys. Status Solidi A*, 2004, **201**, 1302.
4 (*a*) C. Huang, S. Barlow and S. R. Marder, *J. Org. Chem.*, 2011, **76**, 2386; (*b*) R. Schmidt, J. H. Oh, Y.-S. Sun, M. Deppisch, A.-M. Krause, K. Radacki, H. Braunschweig, M. Könemann, P. Erk, Z. Bao and F. Würthner, *J. Am. Chem. Soc.*, 2009, **131**, 6215.
5 (*a*) M. Gsänger, J. H. Oh, M. Könemann, H. W. Höffken, A.-M. Krause, Z. Bao and F. Würthner, *Angew. Chem., Int. Ed.*, 2010, **49**, 740; (*b*) Q. Yan, Y. Zhou, Y.-Q. Zheng, J. Pei and D. Zhao, *Chem. Sci.*, 2013, **4**, 4389; (*c*) Z. Zhang, T. Lei, Q. Yan, J. Pei and D. Zhao, *Chem. Commun.*, 2013, **49**, 2882; (*d*) L. Fan, Y. Xu and H. Tian, *Tetrahedron Lett.*, 2005, **46**, 4443.
6 M.-M. Ling, P. Erk, M. Gomez, M. Koenemann, J. Locklin and Z. Bao, *Adv. Mater.*, 2007, **19**, 1123.
7 (*a*) A. Lv, S. R. Puniredd, J. Zhang, Z. Li, H. Zhu, W. Jiang, H. Dong, Y. He, L. Jiang, Y. Li, W. Pisula, Q. Meng, W. Hu and Z. Wang, *Adv. Mater.*, 2012, **24**, 2626; (*b*) H. Qian, Z. Wang, W. Yue and D. Zhu, *J. Am. Chem. Soc.*, 2007, **129**, 10664.
8 S. Dong, H. Zhang, L. Yang, M. Bai, Y. Yao, H. Chen, L. Gan, T. Yang, H. Jiang, S. Hou, L. Wan and X. Guo, *Adv. Mater.*, 2012, **24**, 5576.
9 (*a*) R. Li, W. Hu, Y. Liu and D. Zhu, *Acc. Chem. Res.*, 2010, **43**, 529; (*b*) H. Usta, A. Facchetti and T. J. Marks, *Acc. Chem. Res.*, 2011, **44**, 501; (*c*) S. Liu, W. M. Wang, A. L. Briseno, S. C. B. Mannsfeld and Z. Bao, *Adv. Mater.*, 2009, **21**, 1217.
10 A. L. Briseno, R. J. Tseng, M.-M. Ling, E. H. L. Falcao, Y. Yang, F. Wudl and Z. Bao, *Adv. Mater.*, 2006, **18**, 2320.
11 (*a*) L. Tan, W. Jiang, L. Jiang, S. Jiang, Z. Wang, S. Yan and W. Hu, *Appl. Phys. Lett.*, 2009, **94**, 153306; (*b*) L. Tan, L. Zhang, X. Jiang, X. Yang, L. Wang, Z. Wang, L. Li, W. Hu, Z. Shuai, L. Li and D. Zhu, *Adv. Funct. Mater.*, 2009, **19**, 272.
12 T. He, M. Stolte and F. Würthner, *Adv. Mater.*, 2013, **25**, 6951.
13 B. A. Jones, A. Facchetti, M. R. Wasielewski and T. J. Marks, *J. Am. Chem. Soc.*, 2007, **129**, 15259.

